Available online at www.sciencedirect.com
ScienceDirect
Journal of Sound and Vibration 311 (2008) 567–578
JOURNAL OF SOUND AND VIBRATION
www.elsevier.com/locate/jsvi

Short Communication

# A note on the periodic and chaotic responses of an SDOF system with piecewise linear stiffness subjected to combined harmonic- and flow-induced excitations

Wang Lin*, Ni Qiao

*Department of Mechanics, Huazhong University of Science and Technology, Wuhan 430074, People's Republic of China*

Received 17 November 2006; accepted 24 August 2007
Available online 23 October 2007

**Abstract**

In this note, the periodic and chaotic responses of two single-degree-of-freedom (SDOF) models are investigated and some interesting results obtained. The first model (original model) has been developed by Narayanan and Sekar [Periodic and chaotic responses of an SDOF system with piecewise linear stiffness subjected to combined harmonic and flow induced excitations, *Journal of Sound and Vibration* 184 (2) (1997) 281–298] and the second one corresponds to a modified system. The original model, involving a one-sided clearance ($y_0$) between the mass and the linear spring, is subjected to combined harmonic ($F\cos\omega t$) and flow-induced excitations. Narayanan and Sekar (1997) has shown that periodic, quasi-periodic and chaotic motions of this original model may occur in a range of flow velocities for the case: $y_0 = 0$ and $F \neq 0$. In the present work, numerical calculations are carried out for several other important cases of the original system, showing some interesting, and sometimes unexpected results. The modified model, in particular, involving both-sided clearances, is analyzed numerically subsequently. The effect of flow velocity, clearances on the global dynamics of this modified system is discussed finally.


## 1. Introduction

Because of their importance in engineering, the dynamic responses of bluff bodies with clearance when subjected to harmonic excitations have been the subject of many investigations. A few examples are given in Ref. [1]. In particular, many bluff bodies are kept in fluid flow. In these cases, the fluid dynamic forces on the structure are nonlinear functions of the velocity of the body in the transverse direction. In flow-induced vibration problems such as aeroelastic flutter, vortex induced and galloping oscillations, and vibrations due to fluid-elastic instability, the aero/fluid dynamic forces inducing the vibrations are almost invariably non-conservative and nonlinear functions of the structural motion, leading to a complex and wide variety of dynamical behaviour characteristic of coupled fluid–structure interaction (FSI) vibrations [2]. Some of the notable contributions in this area were made by Narayanan and Jayaraman [2,3,4] and Simiu and Cook [5].

*Corresponding author. Fax: +86 27 87543238.
*E-mail address:* wanglinfliping@sohu.com (W. Lin).

0022-460X/$ - see front matter 
doi:10.1016/j.jsv.2007.08.021

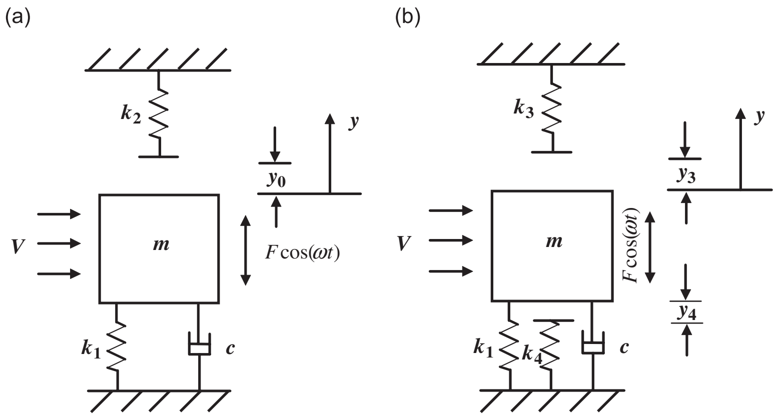


Fig. 1. Two physical models: (a) the original model with one-sided clearance and (b) the modified model with both-sided clearances.

For a perspective on the early study associated with the dynamics of bluff bodies in fluid flow, one can see the book by Blevins [6].

In Ref. [2], the vibrations of a square prism modelled as an single-degree-of-freedom (SDOF) system (see Fig. 1(a)) with unsymmetrical piecewise linear stiffness were investigated under combined harmonic- and flow-induced excitations. The fluid flow normal to the motion of the mass introduces a nonlinear damping force, which is assumed to be characterized by the Blevins [6] square prism model. Thus, the SDOF system represented in Ref. [2] has shown cumulative effects of two different nonlinearities. The first comes from the nonlinear damping force induced by the fluid flow, the second from the nonlinearity due to the impact between the mass and the spring with clearance. Here, it should be stressed that the SDOF system described in Fig. 1(a), involving a one-sided clearance ($y_0$) between the mass and a linear spring, is subjected to combined harmonic- ($F\cos\omega t$) and flow-induced excitations. Based on digital simulations, Narayanan and Sekar [2] have shown that periodic, quasi-periodic and chaotic motions of this SDOF system can be found in a range of flow velocities for the case: $y_0 = 0$ and $F \neq 0$.

In this note, we will further investigate the SDOF system developed in Ref. [2]. The aims of this work are twofold. Firstly, we will represent the dynamical behaviour of the SDOF system with zero or non-zero clearance ($y_0 = 0$ or $y_0 \neq 0$) and without external harmonic excitation ($F = 0$). In this case, the SDOF system (original system) exactly undergoes a flow-induced vibration. The effect of the clearance and the flow velocity on the dynamics of this original system will be analyzed in detail. Secondly, we investigate numerically, yet another modified SDOF system which involving both-sided clearances and subjected to both external harmonic- and flow-induced excitations. It will be shown that rich dynamics occurs in such a modified model. The effects of several key system parameters on the behaviour of this modified model will be discussed finally.

## 2. Background theory

The physical model developed in Ref. [2], which is an SDOF system with one-sided clearance, is shown in Fig. 1(a). The mass $m$ is restrained by a linear spring of stiffness $k_1$ and a dashpot with $c$ as the coefficient of linear viscous damping. When the mass displacement exceeds the clearance $y_0$, the mass will impact onto another linear spring with stiffness $k_2$. Moreover, the mass is assumed to be harmonically excited by an external harmonic excitation of amplitude $F$ and frequency $\omega$. Hence, the equation of motion of the mass under the cumulative effect of two different nonlinearities is given by

$$m\ddot{y} + c\dot{y} + H(y) = F\cos(\omega t) + F_L, \tag{1}$$

in which $F_L$ is the flow-induced force and $H(y)$ represents the nonlinear stiffness function. They have the following formulations, respectively:

$$F_L = \frac{1}{2}\rho S V^2\{B_1(\dot{y}/V) + B_3(\dot{y}/V)^3\}, \quad H(y) = \begin{Bmatrix} k_1 y, & y \leqslant y_0 \\ k_1 y + k_2(y - y_0), & y > y_0 \end{Bmatrix}, \tag{2}$$

where $\rho$ is the density of the flow medium, $S$ the area of the prism facing the flow and $V$ the flow velocity, $B_1$ and $B_3$ are constants, and $t$ represents the time.

As demonstrated in Ref. [2], various periodic motions and chaos can be detected in the original system described in Eq. (1) for the case: $y_0 = 0$ and $F \neq 0$. Moreover, the presence of fluid flow in such an SDOF system results in period-doubling phenomena leading to chaos.

## 3. The SDOF system described in Ref. [2] with one-sided clearance

In this section, the SDOF system in Fig. 1(a) will be further investigated in detail. The nonlinear equation of motion for the SDOF system with external harmonic- and flow-induced excitation may be rendered non-

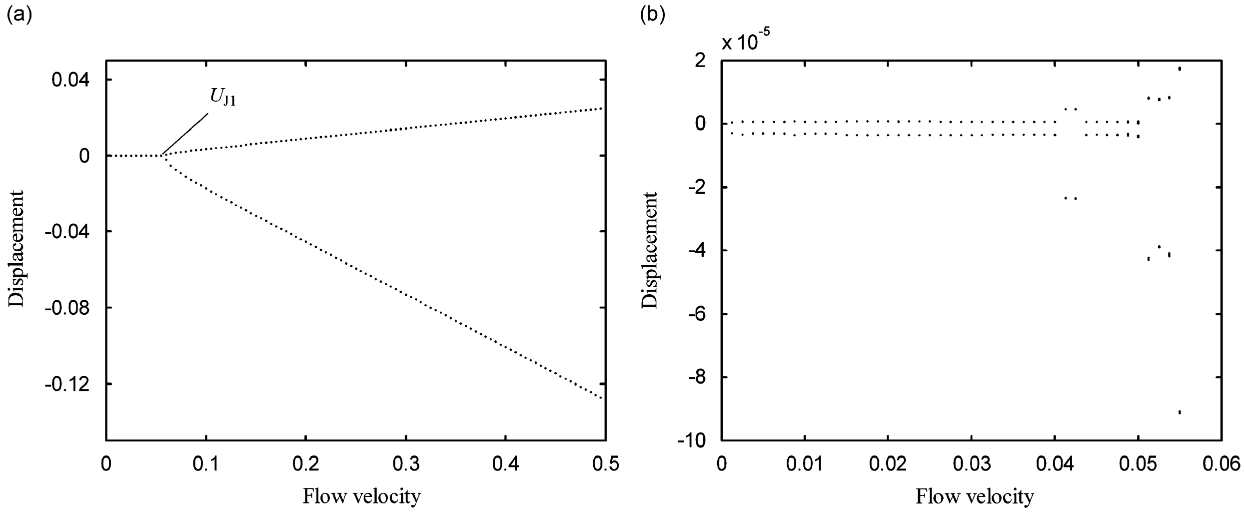


Fig. 2. Bifurcation diagram for the displacement of the original system without external harmonic excitation and $e_0 = 0$: (a) for the range $0 < U < 0.5$ and (b) for a smaller range of $U$.

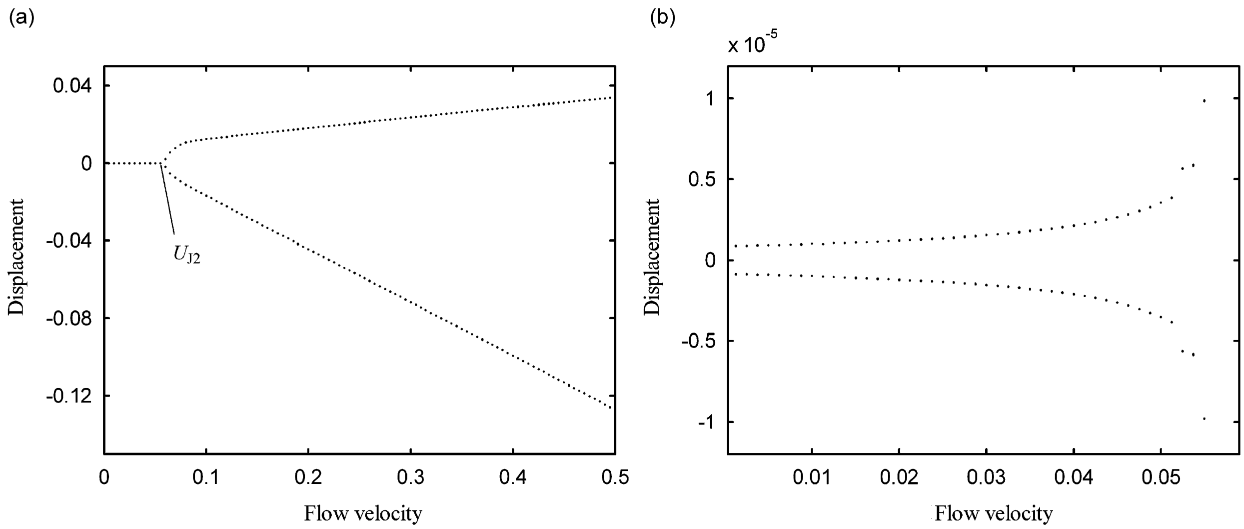


Fig. 3. Bifurcation diagram for the displacement of the original system without external harmonic excitation and $e_0 = 0.01$: (a) for the range $0 < U < 0.5$ and (b) for a smaller range of $U$.

dimensional with the aid of the dimensionless quantities:

$$\sigma = k_2/k_1, \quad x = y/\delta, \quad e_0 = y_0/\delta, \quad \zeta = c/(m\omega_n), \quad U = \rho SV/m\omega_n,$$

$$\tau = \omega_n t, \quad \zeta_1 = -B_1 U/2 \quad \zeta_3 = -\beta^2 B_3/(2U), \quad \beta = \rho S\delta/m,$$

$$\zeta_0 = \zeta + \zeta_1, \quad \Omega = \omega/\omega_n, \quad f = F/(m\omega_n^2\delta),$$

leading to

$$\ddot{x} + \zeta_0\dot{x} + \zeta_3(\dot{x})^3 + h(x) = f\cos(\Omega\tau), \tag{3}$$

where $\omega_n^2 = k_1/m$, $h(x) = x$ when $x \leqslant e_0$ and $= (\sigma+1)x - \sigma e_0$ otherwise. The number of overdots now indicates the order of differentiation with respect to the non-dimensional time $\tau$. If, however, the SDOF system is

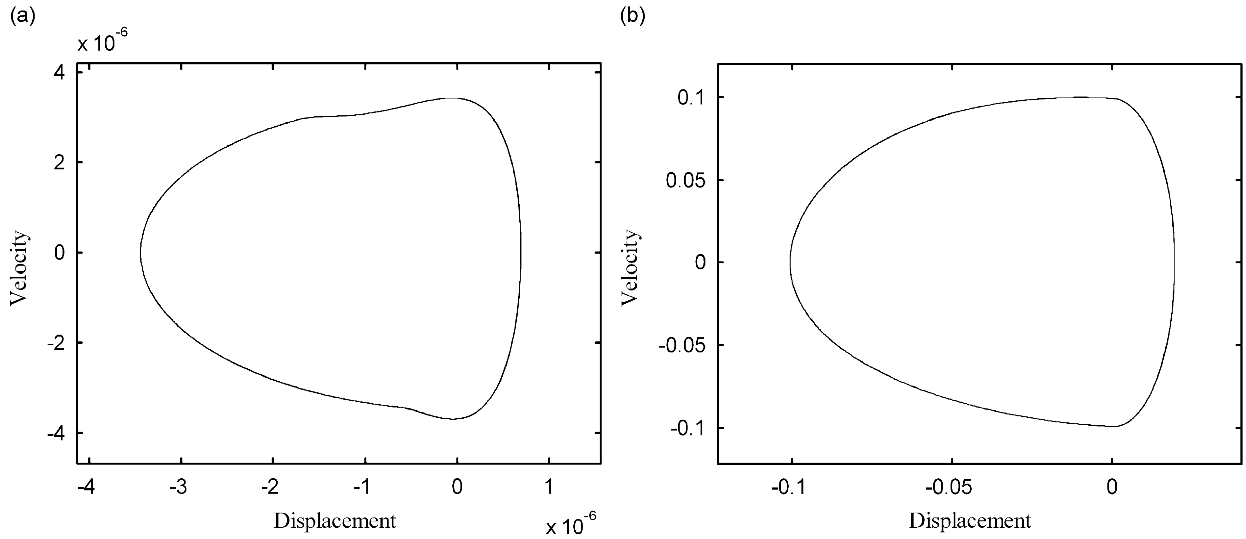


Fig. 4. Phase-plane plots of the original system without external harmonic excitation and $e_0 = 0$: (a) $U = 0.03$ and (b) $U = 0.4$.

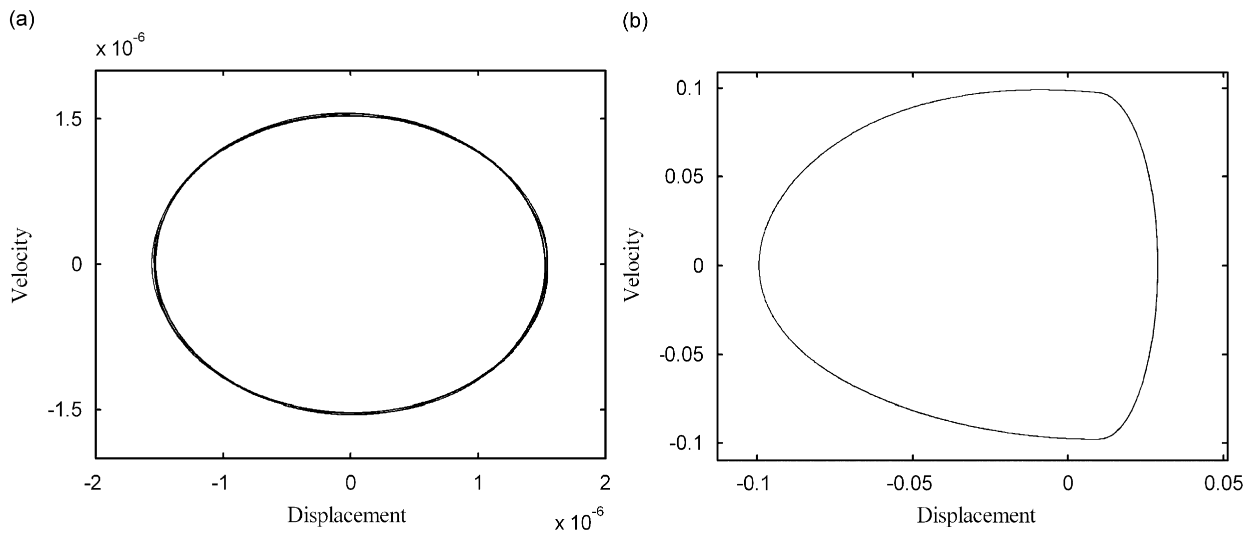


Fig. 5. Phase-plane plots of the original system without external harmonic excitation and $e_0 = 0.01$: (a) $U = 0.03$ and (b) $U = 0.4$.

subjected to no external harmonic excitation, one obtains

$$\ddot{x} + \zeta_0 \dot{x} + \zeta_3 (\dot{x})^3 + h(x) = 0. \tag{4}$$

It should be stressed that some of the above non-dimensional quantities introduced here are different from that described in Ref. [2]. For more details on this aspect one can see Ref. [2]. In what follows of this section, numerical simulations will be carried out and some typical dynamics of the SDOF system considered will be shown.

### 3.1. Without external harmonic excitation for $e_0 = 0$ or $e_0 \neq 0$

Here, it should be mentioned that various behaviour of this system has, of course, been studied before by Narayanan and Sekar [2], but only for the case $y_0 = 0$ and $F \neq 0$. In this short communication, firstly, we will consider the dynamics of this SDOF system with $y_0 = 0$ (or $y_0 \neq 0$) and $F = 0$. This system is exactly corresponding to a flow-induced vibration problem.

Solutions of Eq. (4) were obtained by using a fourth-order Runge–Kutta integration algorithm, where a novel approach for solving dynamical systems with motion dependent discontinuities [7] was also utilized.

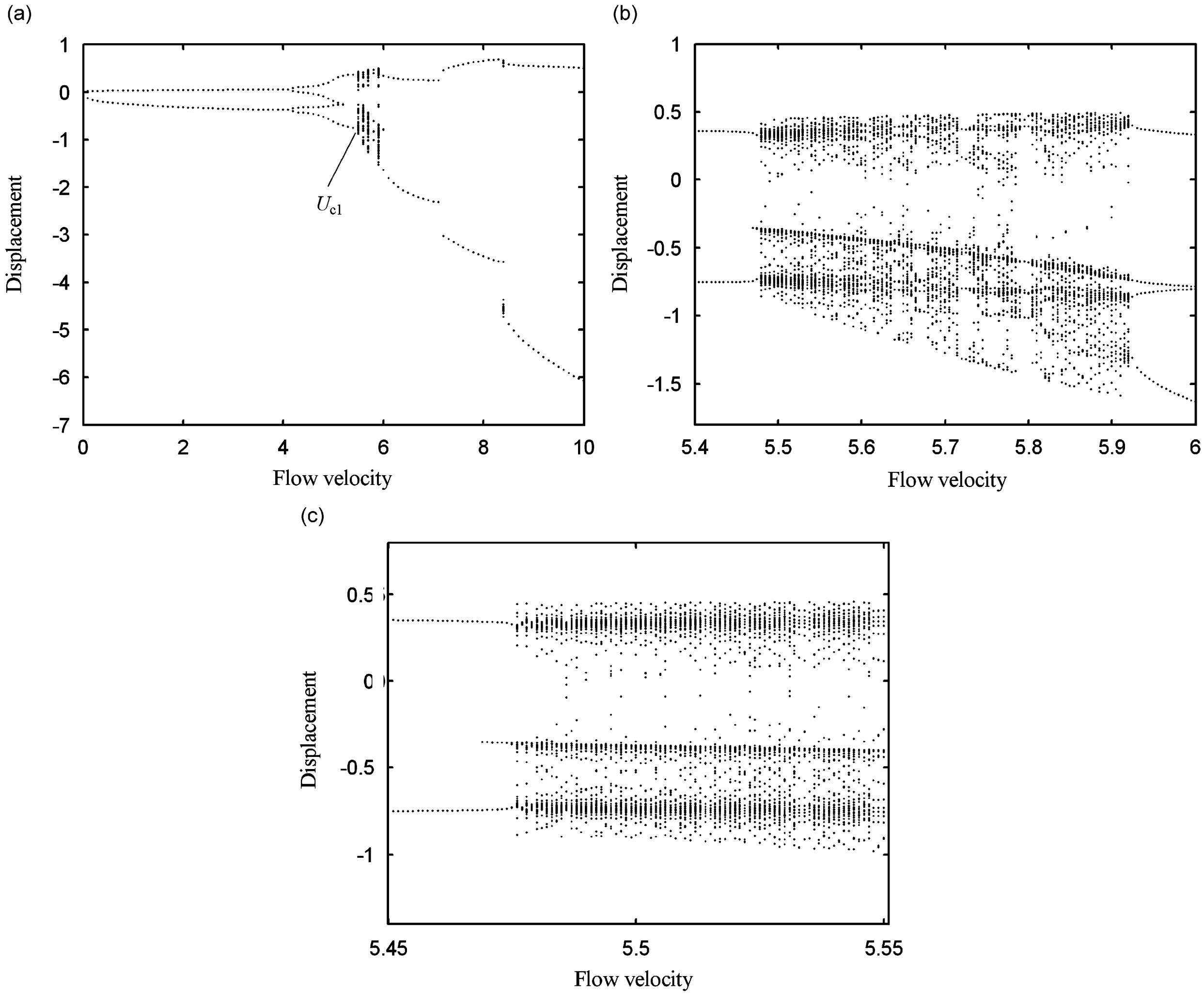


Fig. 6. Bifurcation diagram for the displacement of the original system with external harmonic excitation and $e_0 = 0.0$, $f = 5$, $\Omega = 5$: (a) for the range $0 < U < 10$ and (b, c) for two smaller ranges of $U$.

The initial conditions employed were $x(0) = 0.001$, $\dot{x}(0) = 0$. Based on this integration algorithm, numerical calculations have produced the bifurcation diagram of Figs. 2 and 3, as the flow velocity ($U$) is varied in the range $0 \leqslant U \leqslant 0.5$, and the values of several other parameters are fixed to be $\sigma = 25$, $\zeta = 0.05$, and $\beta = 1$.

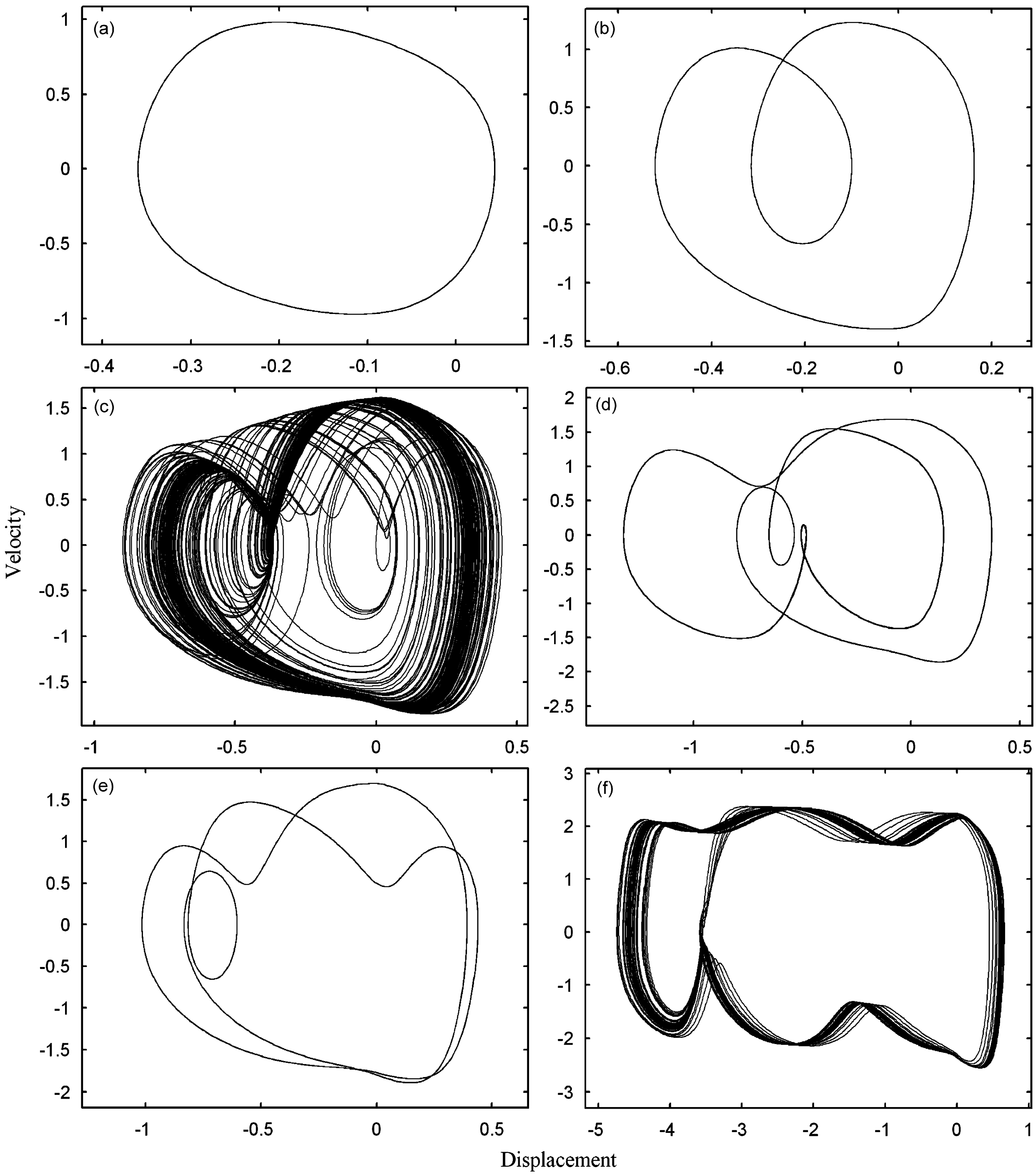


Fig. 7. Phase-plane plots of the original system with external harmonic excitation and $e_0 = 0.0$, $f = 5$, $\Omega = 5$: (a) $U = 2.0$, (b) $U = 4.8$, (c) $U = 5.5$, (d) $U = 5.725$, (e) $U = 5.795$, and (f) $U = 8.4$.

The constants $B_1$ and $B_3$, which depend on the geometry of the bluff body, are taken as 2.7 and −31.0, respectively [6].

It can be seen from Figs. 2 and 3 that the variable parameter is the dimensionless flow velocity $U$. In Fig. 2, the clearance between the mass and the spring of $k_2$ is chosen to be zero ($e_0 = 0$); In Fig. 3, however, the clearance between the mass and the spring of $k_2$ is chosen to be non-zero (e.g., $e_0 = 0.01$). From these two figures, it can be seen that the system always undergoes a period-1 motion in the range of $0 \leqslant U \leqslant 0.5$, which is corresponding to the case $f = 0$. Here, a result of interest is related to the vibrating amplitudes. As represented in the bifurcation diagram of Fig. 2, a jump point noted at $U = U_{J1}$ occurs. In the vicinity of this jump point, the vibrating amplitudes of the system change sharply. When $U < U_{J1}$ the non-dimensional vibrating amplitudes of the system are very small (magnitude:$10^{-6}$). However, if $U > U_{J1}$, the vibrating amplitudes of the system become much larger (magnitude:$10^{-2}$), which is clearly visible in Fig. 2. The nature of this interesting

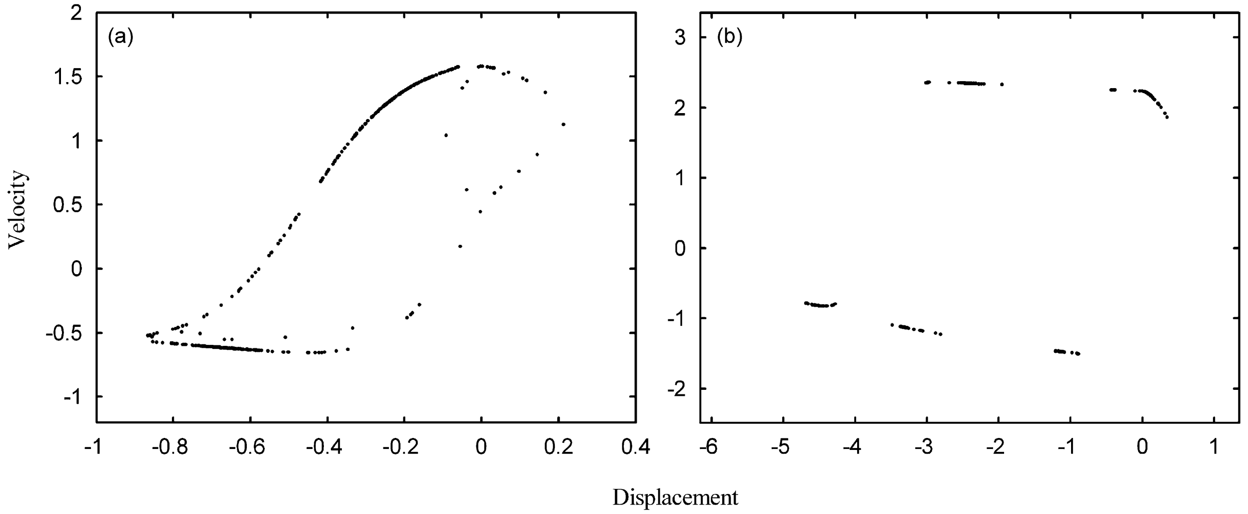


Fig. 8. Poincare maps of the original system with external harmonic excitation and $e_0 = 0.0$, $f = 5$, $\Omega = 5$: (a) $U = 5.5$ and (b) $U = 8.4$.

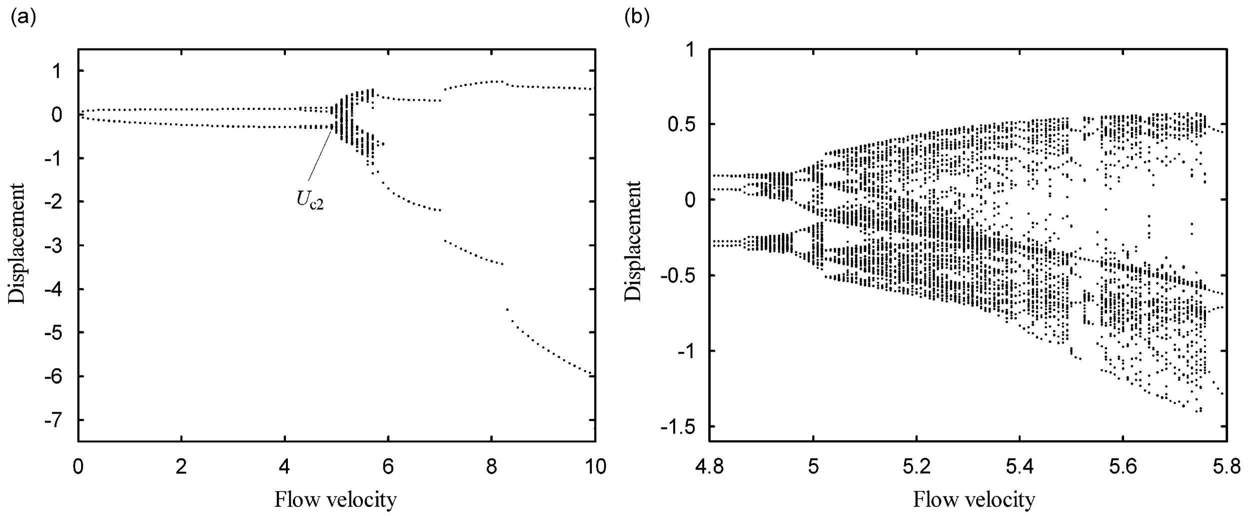


Fig. 9. Bifurcation diagram of the original system with external harmonic excitation and $e_0 = 0.1$, $f = 5$, $\Omega = 5$: (a) for the range $0 < U < 10$ and (b) for a smaller range of $U$.

phenomenon is not understood yet. Moreover, if $e_0 = 0.01$, a similar jump point can be detected, which is denoted at $U = U_{J2}$ in Fig. 3. The second result of interest is related to the clearance, $e_0$. From Figs. 2 and 3, one can obviously see that $U_{J1} = U_{J2}$. In fact, even with large values of clearance (e.g., $e_0 = 0.2$), the threshold flow velocity (denoted to be $U_{Ji}$) for the jump point is very close to the value of $U_{J1}$. Hence, the global dynamics of system (4) in the parameter range of flow velocity is not sensitive to $e_0$.

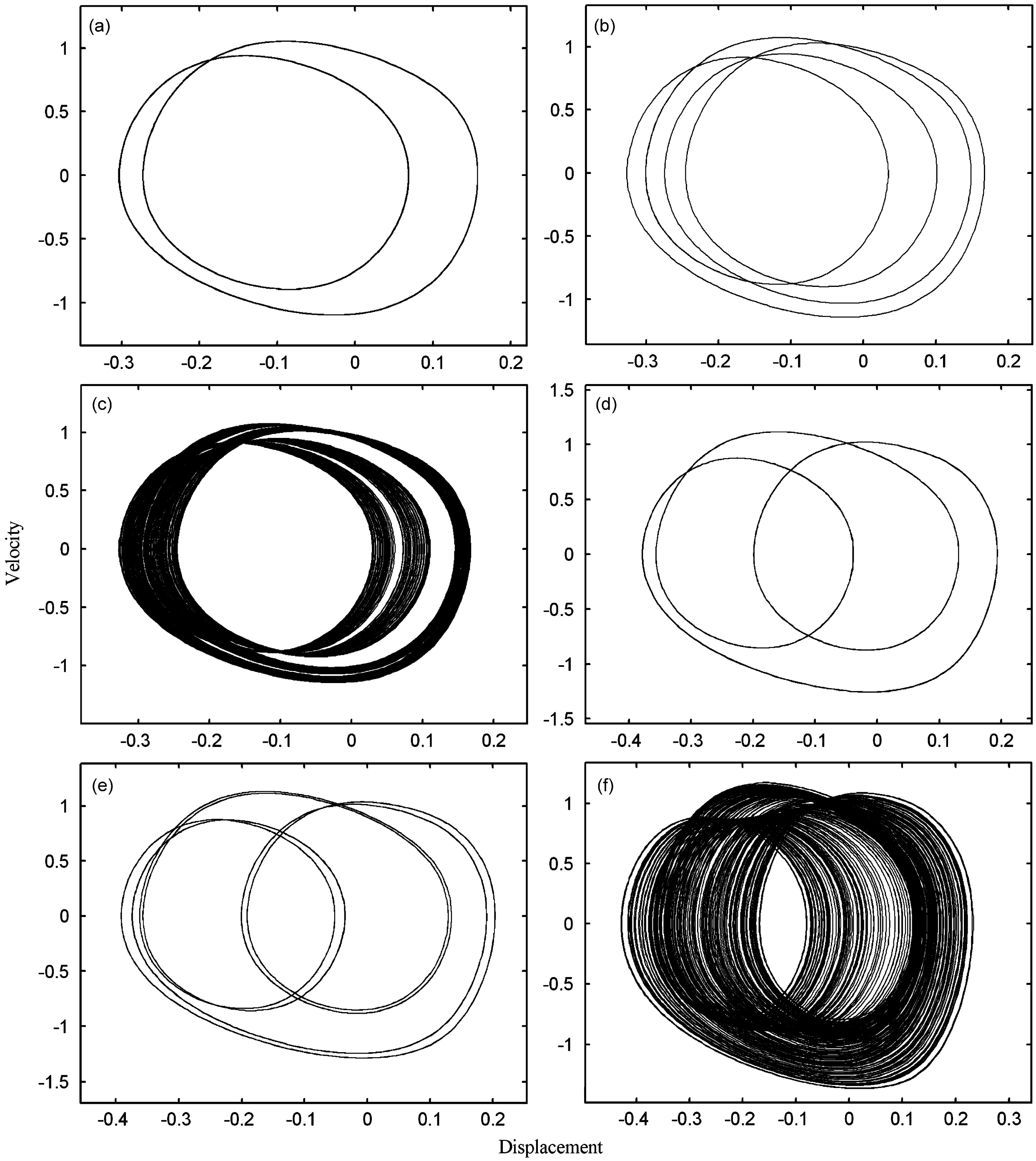


Fig. 10. Phase-plane plots of the original system with external harmonic excitation and $e_0 = 0.1$, $f = 5$, $\Omega = 5$: (a) $U = 4.82$, (b) $U = 4.88$, (c) $U = 4.90$, (d) $U = 4.977$, (e) $U = 4.985$, and (f) $U = 4.995$.

It is instructive to look at phase-plane portraits associated with several values of $U$, corresponding to the dynamical behaviour as discussed in the foregoing. Sample results are shown in Figs. 4 and 5. Here, it is noted that, no other motions (e.g., period-$n$ ($n>1$), quasi-periodic or chaotic motions) have been detected even with sufficiently high flow velocities.

### 3.2. With external harmonic excitation for $e_0 = 0$ or $e_0 \neq 0$

To analyze the forced vibrations of the SDOF system shown in Fig. 1(a), solutions of Eq. (3) were obtained via numerical simulations. In what follows of this subsection, several key parameters are chosen to be $\sigma = 25$, $\zeta = 0.05$, $\beta = 1, f = 5$, and $\Omega = 5$. In this case, the external harmonic excitation is non-zero. It is observed that system (3) may represent much richer dynamical behaviour than system (4), both for $e_0 = 0$ and $e_0 \neq 0$. For $e_0 = 0$, the oscillations of the mass are periodic for $U<5.48$ and are also periodic for $U>5.92$. This clearly appears in the bifurcation diagrams of Fig. 6(a). However, indeed, at $U = U_{c1} = 5.48$, chaos, followed by a period-2 motion, arises. Sample results of phase-portrait plots and Poincare maps are shown in Figs. 7 and 8 for various values of $U$. In this case there are relatively small regions of periodic motions embedded within the chaotic region; e.g., for $5.794<U<5.802$ there is what appears to be a period-4 region. Moreover, in the vicinity region of $U = 8.40$, chaotic motion can be detected, as shown in Figs. 7(f) and 8(b).

Similar results can be obtained for the case $e_0 \neq 0$. However, the threshold flow velocity for the onset of chaos is $U_{c2} = 4.9$, which is much lower than that for the case $e_0 = 0$. Moreover, the bifurcation details in the vicinity of $U_{c2}$ are also different. From the expanded version of the bifurcation diagram for a smaller range of $U$, a sequence of period-doubling bifurcations is clearly visible (see Fig. 9(b)). It ought to be remarked that several series of period-doubling bifurcations can be found with increasing $U$ (see the evolution of phase-plane plots in Fig. 10). Thus, with external harmonic excitation, the effect of clearance, $e_0$, on the global dynamics of system (3) is significant.

## 4. Another SDOF system with both-sided clearances

In this section a modified SDOF system shown in Fig. 1(b) will be considered. It can be seen that this modified system has both-sided clearances. The stiffness of the two springs with clearances is denoted as $k_3$ and $k_4$, respectively. The clearances between the mass and the springs are $e_3$ and $e_4$. In what follows, $e_3$ and $e_4$ may be different from each other in the numerical calculations.

Similarly, by considering the effects of both-sided clearances, the nonlinear equation of motion of this modified SDOF system can be written as

$$m\ddot{y} + c\dot{y} + G(y) = F\cos(\omega t) + F_L, \tag{5}$$

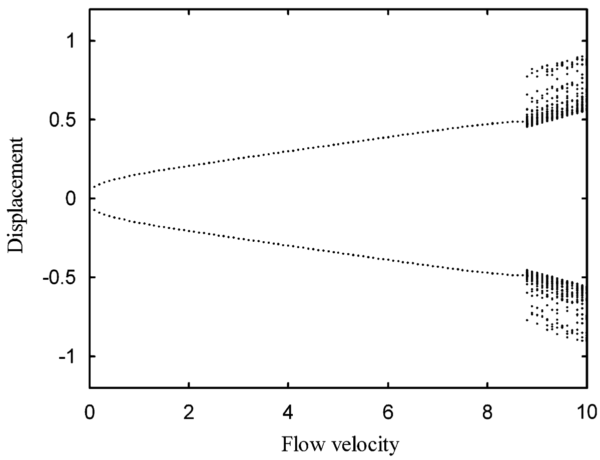


Fig. 11. Bifurcation diagram of the modified system with external harmonic excitation and $e_3 = 0.1$, $e_4 = 0.1$, $f = 5$, $\Omega = 5$, as $U$ is varied.

in which

$$F_L = \frac{1}{2}\rho S V^2\{B_1(\dot{y}/V) + B_3(\dot{y}/V)^3\}, \quad G(y) = \left\{\begin{array}{ll} k_1 y, & -y_4 \leqslant y \leqslant y_3 \\ k_1 y + k_3(y - y_3), & y > y_3 \\ k_1 y + k_4(y + y_4), & y < -y_4 \end{array}\right\}. \tag{6}$$

Similarly, upon introducing the following non-dimensional parameters:

$$\sigma_3 = k_3/k_1, \quad \sigma_4 = k_4/k_1, \quad x = y/\delta, \quad e_3 = y_3/\delta, \quad e_4 = y_4/\delta, \quad \zeta = c/(m\omega_n),$$

$$U = V/(\delta\omega_n), \quad \tau = \omega_n t, \quad \zeta_1 = -\beta B_1 U/2, \quad \zeta_3 = -\beta B_3/(2U),$$

$$\beta = \rho S\delta/m, \quad \zeta_0 = \zeta + \zeta_1, \quad \Omega = \omega/\omega_n, \quad f = F/(m\omega_n^2\delta).$$

Eq. (6) becomes

$$\ddot{x} + \zeta_0\dot{x} + \zeta_3(\dot{x})^3 + g(x) = f\cos(\Omega\tau), \tag{7}$$

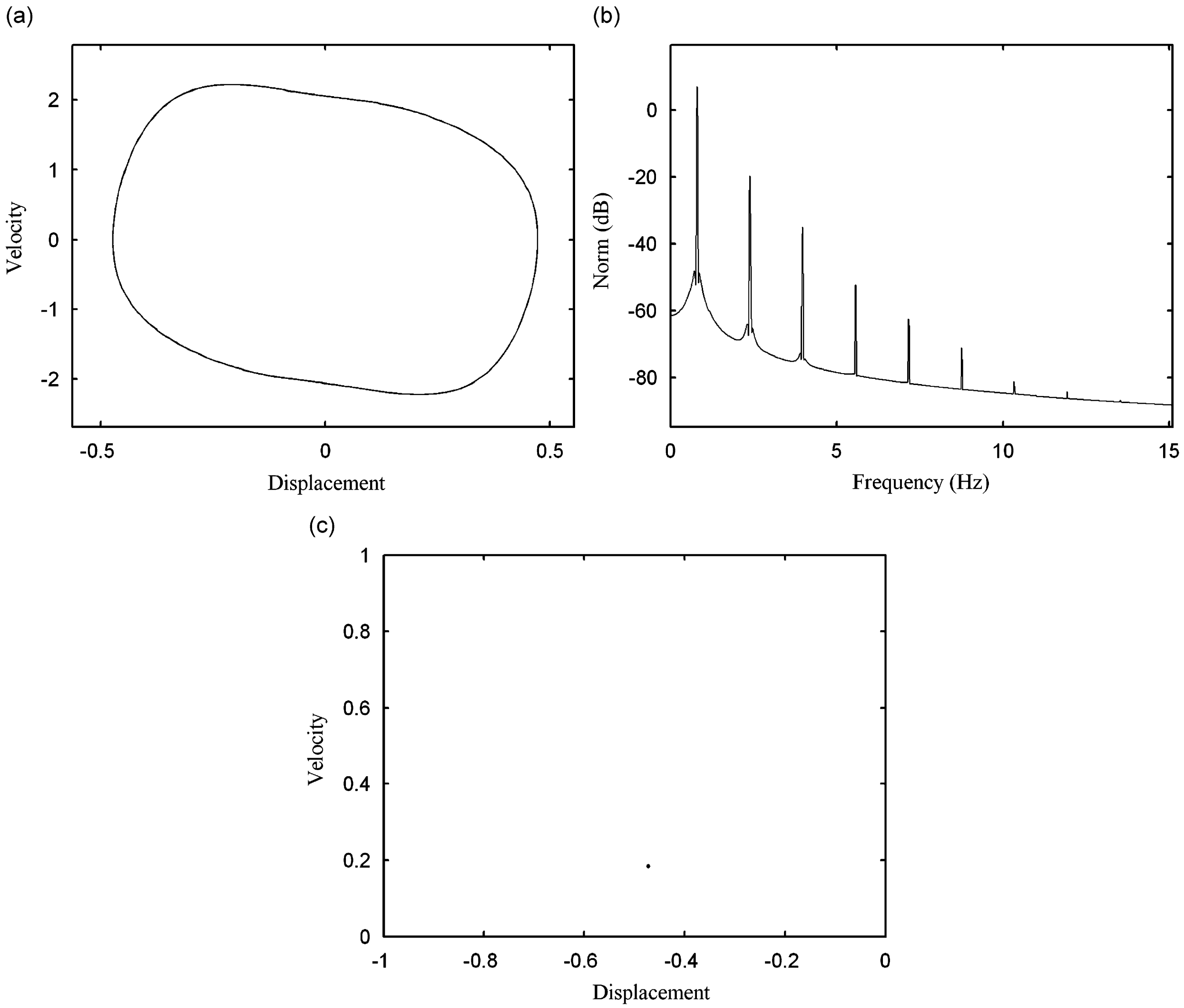


Fig. 12. Phase-plane plot, power spectra and Poincare map of the modified system with external harmonic excitation and $e_3 = 0.1$, $e_4 = 0.1$, $f = 5$, $\Omega = 5$, for $U = 8.0$.

where

$$g(x) = \left\{ \begin{array}{ll} x, & -e_4 \leqslant x \leqslant e_3 \\ x + \sigma_3(x - e_3), & x > e_3 \\ x + \sigma_4(e + e_4), & x < -e_4 \end{array} \right\}. \tag{8}$$

Similarly as before, solutions of Eq. (7) were obtained by using a fourth-order Runge–Kutta method, with the same initial conditions employed in the foregoing. The parameters are selected to be $\sigma_3 = \sigma_4 = 25$, $\zeta = 0.05$, $\beta = 1$, $f = 5$, and $\Omega = 5$. Some typical results are summarized in Figs. 11–14. Fig. 11 shows the bifurcation diagram where the maximum tip displacements are plotted as functions of the flow velocity $U$. It is observed that, after the region of period, the system becomes quasi-periodic. Fig. 13 confirms this quasi-periodic motion via PSD diagram and Poincare map. It ought to be remarked that Figs. 11–13 are obtained with $e_3 = e_4 = 0.1$.

More calculations were performed also when $e_3$ is chosen to be the variable parameter. Similar bifurcation diagram can be constructed, as shown in Fig. 14. In this case, it is interesting to note that for $e_3 < 0.0897$, the system undergoes a period-1 motion; however, for $e_3 > 0.0897$, quasi-periodic motion occurs.

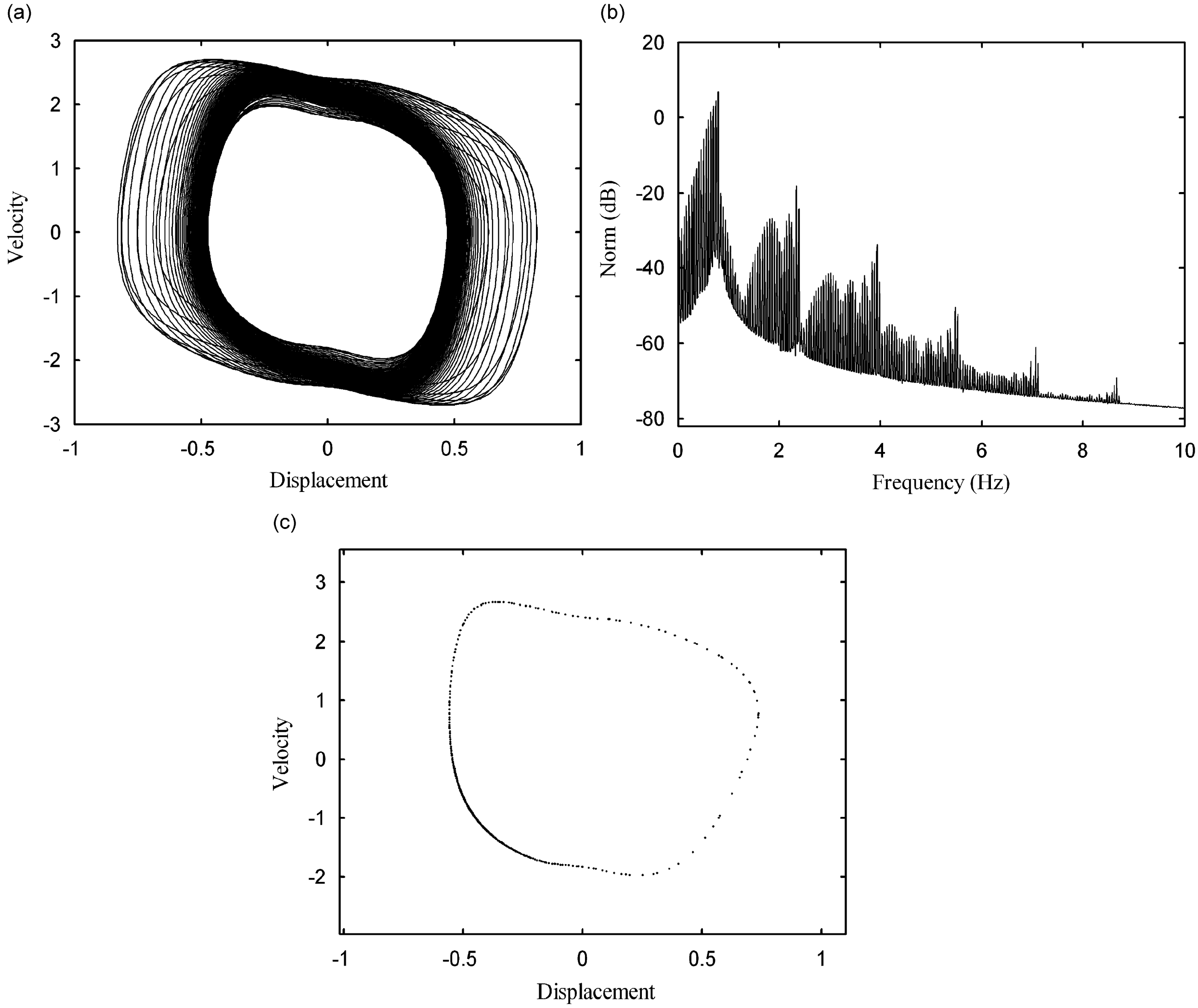


Fig. 13. Phase-plane plot, power spectra and Poincare map of the modified system with external harmonic excitation and $e_3 = 0.1$, $e_4 = 0.1$, $f = 5$, $\Omega = 5$, for $U = 9.0$.

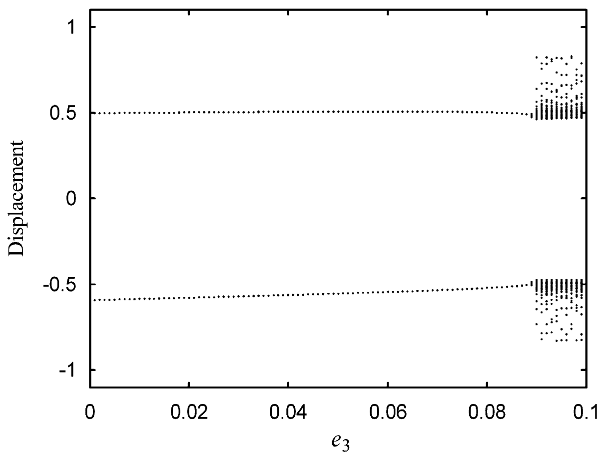


Fig. 14. Bifurcation diagram of the modified system with external harmonic excitation and $U = 9.0$, $e_4 = 0.1$, $f = 5$, $\Omega = 5$, as $e_3$ is varied.

## 5. Discussion

In this short communication, the nonlinear dynamics of the SDOF system described in Ref. [2] and another modified system, both with and without external harmonic excitation, was explored numerically. Moreover, this is a multidimensional investigation of the effects of (i) the impact models with springs and clearances and (ii) the nonlinearity of the type associated with the flow-induced excitation.

The dynamical behaviour was analyzed for two models. For the original model with one-sided clearance, attention was concentrated on the flow-induced vibrations of this SDOF system, both with and without external harmonic excitation. In this case, we have also discussed the effect of the clearance ($e_0 = 0$ and $e_0 \neq 0$) on the global dynamics of this one-sided model. Then another modified model with both-sided clearances was developed and numerically analyzed. The differences of the dynamical behaviour between these two models can be clearly found. In the parameter range of flow velocity $0 < U < 10$, chaos, followed by a series of period-doubling bifurcations, arises, for the one-sided model with non-zero clearance. However, for the both-sided model, only period-1 and quasi-periodic motions were detected in the range $0 < U < 10$. Whether this both-sided model can represent chaos or not should be further investigated via theoretical and numerical analysis.

## References

[1 G. Schmidt, A. Tondl, *Non-Linear Vibrations*, Cambridge University Press, Cambridge, 1986.

[2] S. Narayanan, P. Sekar, Periodic chaotic responses of an SDOF system with piecewise linear stiffness subjected to combined harmonic, flow induced excitations, *Journal of Sound and Vibration* 184 (2) (1997) 281–298.

[3] K. Jayaraman, S. Narayanan, Periodic and chaotic oscillations of a harmonically excited square prism in fluid flow, *Proceedings of the National Seminar on Aerospace Structures, India* (1990) 181–191.

[4] S. Narayanan, K. Jayaraman, Chaotic oscillations of a square prism in fluid flow, *Journal of Sound and Vibration* 166 (1993) 87–101.

[5] E. Simiu, G.R. Cook, Chaotic motions of self excited forced and autonomous square prisms, *Proceedings of the American Society of Civil Engineers, Journal of the Engineering Mechanics Division* 117 (1991) 241–259.

[6] R.D. Blevins, *Flow-induced Vibration*, Van Nostrand Reinhold, New York, 1977.

[7] M. Wiercigroch, Modelling of dynamical systems with motion dependent discontinuities, *Chaos, Solitons and Fractals* 11 (2000) 2429–2442.